ISSN 2682-681X (Paper), ISSN 2705-4241 (Online) | http://unilorinjoger.com | https://doi.org/10.63745/jogersi.2026.06.30.007

JOGER SPECIAL ISSUE, 2026
JOURNAL OF GEOMATICS AND ENVIRONMENTAL RESEARCH http://www.unilorinjoger.com

Mapping of Land Use/Land Cover Dynamics and Land Surface Temperature in Osogbo, Osun State, Nigeria

[1]Nwodo, G. O., [2*]Tata H, [3]Nnamani O. J.

[11]Department of Geomatics, Faculty of Environmental Sciences, University of Benin, Benin City, Edo State, Nigeria
[2,3]Department of Surveying and Geoinformatics, Federal University of Technology Akure, Ondo State, Nigeria

*htata@futa.edu.ng | https://orcid.org/0000-0002-9755-1612

Abstract

Change in land use and land cover (LULC) is one of the most obvious pieces of evidence of human modification on the earth's surface. The Land use and land cover of Osogbo over the last 30 years were analyzed to determine the effects of Land use and land cover changes on both Temperature and Vegetation. Landsat imagery from 1991, 2001, 2011, and 2021 was used to analyze Land use and land cover change using a supervised image classification method. The LST was found to have a continuous increase, most especially within the area with increasing settlement, while the NDVI was on the decline. The correlation between the LST, Settlements, and NDVI shows that there is a very strong positive correlation between the LST and Settlements (r = 0.80), while there exists a very weak negative correlation between the NDVI and Settlements (r = -0.04) within the study area. Correlation analysis further shows that although thick vegetation cover increased over the period, it remained only weakly related to NDVI (r = -0.19), whereas light vegetation cover, which declined markedly over the same period, showed a very strong negative correlation with NDVI (r = -0.93). This indicates that the observed expansion in vegetated area is not necessarily accompanied by an improvement in vegetation health, and that much of the remaining light vegetation cover in the study area may be degraded or under stress. It is therefore recommended that an environmental impact assessment be carried out within the study area.

ARTICLE INFORMATION
Received: 20 May 2026
Revised: 25 May 2026
Accepted: 29 May 2026
Published: 20 July 2026

KEYWORDS
Geospatial Mapping
Land Use;
Land Cover;
Land Surface Temperature

Citation: Nwodo, G. O., Tata H, & Nnamani O. J. (2026). Geospatial Mapping of Land Use/Land Cover Dynamics and Land Surface Temperature in Osogbo, Osun State, Nigeria. *Journal of Geomatics and Environmental Research*, Special Issue 1(1), Pp 90-102.

1. INTRODUCTION

Change in Land Use and Land Cover (LULC) is one of the most obvious pieces of evidence of human modification on the Earth's surface, and it has a first-order control on the thermal characteristics of urban and peri-urban landscapes. The conversion of natural vegetated, areas and open lands (agricultural land, wetland) to impervious built-up and bare surfaces for the support of increasing population and the urban expansion significantly modify the radiative, thermal, and moisture characteristics of land surface and result in higher surface temperature and a significant Urban Heat Island (UHI) phenomenon for many cities (Weng, 2001; Voogt & Oke, 2003; Arnfield, 2003). UHI has been the central theme of research in urban climatology, urban environmental planning, and urban sustainability since heat stress increases the risk to human lives and buildings of facing climatic extremes and requires more cooling energy. Meanwhile, the UHI increases the likelihood of urban pollutant formation and adversely affects the health and comfort of urban populations (Shi *et al.,* 2021; Stewart *et al*., 2021).

Nowadays, satellite-based thermal infrared remote sensing can provide surface temperature estimates for large-scale, spatially coherent areas, even where ground measurements are absent, as a complement to sparse meteorological observations. By processing of Brightness Temperature (BT) from Landsat series, MODIS and other thermal imaging sensors through, for example, the mono-window algorithm (Becker & Li, 1990), the single-channel algorithm (Yu *et al.,* 2014), and the split-window algorithm (Du *et al*., 2015), Land Surface Temperature (LST) can be obtained with acceptable accuracy and different spatial resolutions and input requirement levels. The satellite data can usually be processed with readily available tools and at relatively low cost due to standardization, uniformity of sensors, open access to data and processing algorithms, and uniformity of sensor data standards (Chander *et al.,* 2009), so it has become a routine task of estimating LST over vast regions in both developed and developing countries.

Indeed, numerous studies indicate that spatial variations in LST are significantly linked to the composition and configuration of LULC.

Pioneering work in this field, such as Weng (2001), examined LULC change in China's Zhujiang Delta and identified a strong positive association between urban growth and increased surface temperatures. Subsequent studies confirmed correlations between impervious surface cover and higher surface temperatures. Building on Weng's contribution, research using data from other study areas and approaches, such as Weng et al. (2004) on vegetation fraction as a cooling factor and Weng et al. (2007) on land cover configuration as determinants of the UHI, further explored and refined additional factors controlling land surface temperatures. The relationship is so strong that Weng (2003) even used fractal methods to describe the structure of the UHI in the Zhujiang Delta, arguing that simple LULC proportions alone could not fully capture the UHI phenomenon.

Spectral indices from optical sensors have been widely used to operationalize the relationship between LULC and LST. Common indices include the Normalized Difference Vegetation Index (NDVI) (Rouse et al., 1974), which is generally negatively related to LST due to the thermal cooling of transpiring vegetation, and the Normalized Difference Built-up Index (NDBI) (Zha et al., 2003), which is positively correlated with LST and often represents impervious surfaces. Numerous studies, such as those by Guha et al. (2018) in two Italian cities, have reported negative correlations of LST with NDVI and positive correlations of LST with NDBI; however, these correlations weaken markedly within urban core regions, suggesting limitations of index-based methods for within-urban analyses of the thermal environment. For instance, Karnieli et al. (2010) showed that the NDVI–LST relationship is sensitive to background soil moisture and vegetation phenology and should be interpreted with caution in drought-prone or semi-arid environments.

Going beyond bivariate correlations, several studies have attempted to measure more holistic determinants of the surface urban heat island (e.g., urban size, population density, development intensity, and the percentage of water bodies) and have tended to reveal strong positive correlations with the extent of the built environment and weak negative correlations with the percentage of vegetated area and water coverage (Cai et al., 2016). Following the call for more mechanistic approaches to estimating surface emissivity, atmospheric correction, and energy balance to move beyond simple correlation analyses (Voogt and Oke, 2003), subsequent work has focused on developing advanced algorithms and multi-sensor fusion techniques (Parlow, 2021; Shi et al., 2021). Further work by Stewart et al. (2021) illustrated how the surface urban heat island changes with the evolving growth pattern of urban expansion, suggesting that a time-change-based spatial method may offer more insightful perspectives than a single-date view.

A global review of LULC-LST interactions conducted by Nega and Balew (2022) also concluded that built-up land has the highest LST, followed by bare land, whereas water bodies and dense vegetation generally have the lowest LST across climatic zones and geographical regions.

As a consequence of this globally consistent directional relationship between LULC and LST, numerous case studies at local scales have been conducted, particularly in highly urbanized regions, including many cities in the Global South. For example, in Nigeria, studies showed an increasing intensity of LST in Lagos Metropolis between 1984 and 2013 due to rapid urban expansion over natural and semi-natural surfaces (Babalola and Akinsanola, 2016); over Ekiti State, also in Nigeria, in the last 45 years (Olorunfemi *et al.,* 2018); in Ibadan, also in Nigeria (Fashae *et al.,* 2020); and over Benin City, where local warming has been attributed primarily to land cover changes (Fabolude and Aighewi, 2022). The case studies collectively show that, although the direction of the relationship between LULC and LST is generally consistent across the globe, its intensity can vary with urban context, including regional climate, physical urban structure, and the rate of land-use change. Despite this extensive body of research, several gaps remain.

Most existing studies either used single- or two-date comparative analyses that do not fully capture LULC-LST evolution trends, or did not adequately couple high-accuracy LULC mapping results with statistical analyses.

Geographically, research has been predominantly focused on East Asia and North America, and on many cities, with a scarcity of high-resolution, time-series, remote-sensing-based analyses in rapidly expanding cities in Africa, where the consequences of surface warming, such as thermal stress and heat-related health outcomes, could be more acute. In this research, we therefore employ a spatiotemporal approach using remote sensing and Geographic Information Systems to map and assess LULC changes and their influence on LST, and to quantify the statistical relationship between LULC classes and LST dynamics in the study area, providing an empirical basis for informed land-use planning, green infrastructure policy development, and climate adaptation strategies.

Specifically, the objectives of this study were to: (i) classify and quantify land use/land cover changes in Osogbo Local Government Area between 1991 and 2021 using multi-temporal Landsat imagery; (ii) derive and map the spatiotemporal pattern of Land Surface Temperature (LST) across the same period; (iii) generate the Normalized Difference Vegetation Index (NDVI) as a proxy for vegetation cover and health; and (iv) statistically evaluate the relationships among LULC classes, LST, and NDVI to determine the extent to which urban expansion has modified the local thermal and vegetation environment. All four Landsat scenes (1991, 2001, 2011, and 2021) used in this study were acquired during the dry season (December-January) to minimize the confounding effects of seasonal phenology and cloud cover on the derived LST and NDVI values.

2. MATERIALS AND METHODS

2.1 The Study Area

Osogbo, the capital of Osun State, is located in southwestern Nigeria at latitude 7°48'00" N and longitude 4°35'00" E. Osogbo borders Ede, Olorunda, Obokun, Egbedore, Orolu, Ifelodun, Boripe, Atakumosa, and Ilesa. Precipitation varies by 193 cm between the driest and wettest months. The annual temperature varies by approximately 4.6°C. Osogbo serves as the administrative and commercial hub of Osun State. Since Osun State's creation, Osogbo has experienced significant population growth. Under the current government (2011 to present), there has been considerable road expansion and construction, leading to increased urbanization and population growth in Osogbo and its suburbs.

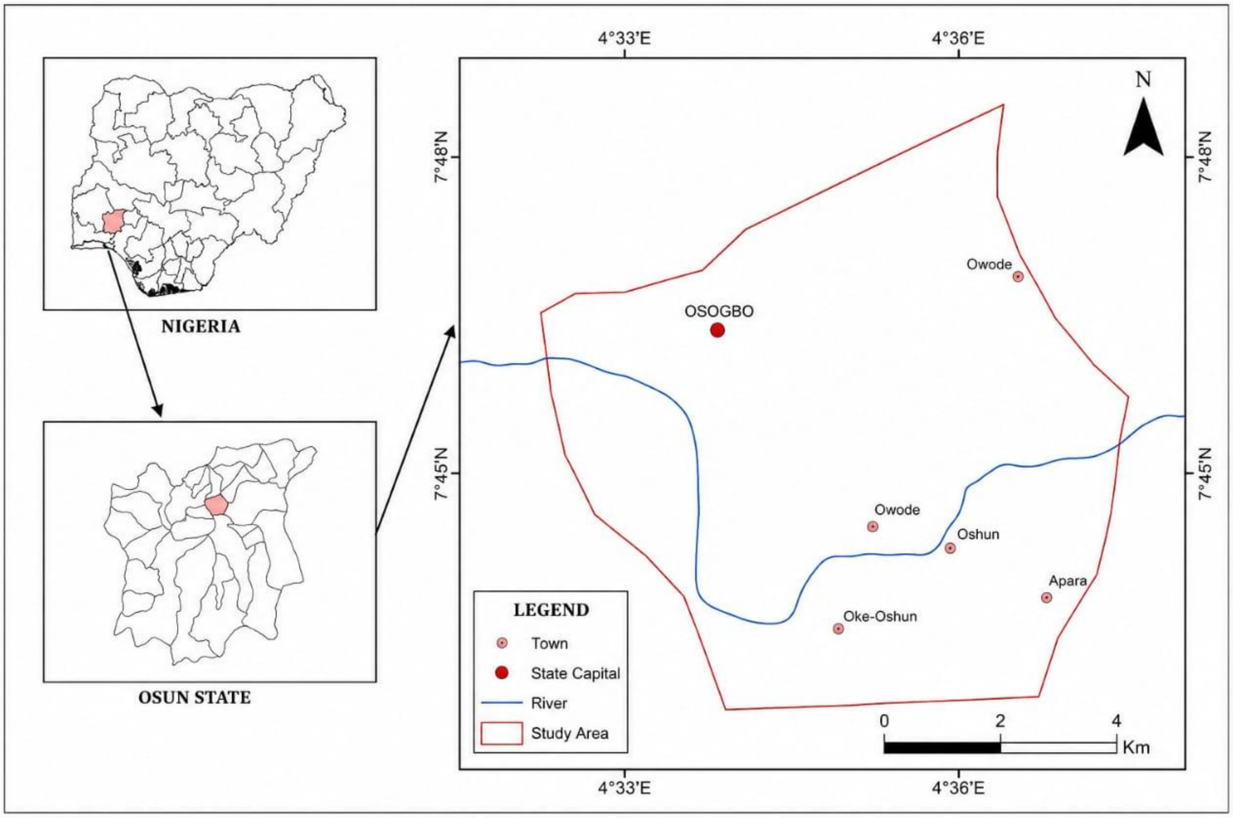

Figure 1. Study Area showing LGAs in Osun State (source: Authors, 2026)

2.2 Data Processing

The Landsat image series used in this study included Landsat 4 and 5 for 1991 and 2001, Landsat 7 for 2011, and Landsat 8 for 2021. Supervised image classification was used to determine land-use and land-cover changes over time, using a near-infrared color combination (Band 4, 3, 2 for Landsat 4, 5, and 7, and Band 5, 4, and 3 for Landsat 8) with the composite tool in ArcGIS 10.8.

Before classification, all scenes were radiometrically calibrated to top-of-atmosphere reflectance and geometrically co-registered to a common Universal Transverse Mercator (UTM Zone 31N, WGS 1984) reference frame to ensure comparability across dates. For the 2011 Landsat 7 ETM+ scene, the Scan Line Corrector (SLC)-off data gaps were filled using the focal/local-window gap-fill approach in ArcGIS before classification, and areas with residual striping were excluded from the accuracy assessment sample. Classification accuracy for each of the four epochs was evaluated using a stratified random sample of reference points on high-resolution imagery.

The overall classification accuracy for 1991, 2001, 2011, and 2021 was 0.65, 0.83, 0.90, and 0.77, respectively, while the kappa coefficient was 0.53, 0.77, 0.86, and 0.68, respectively, for the study period.

2.3 Land Surface Temperature (LST) Change

The land surface temperature (LST) of the study area was derived from satellite imagery using the thermal bands (Band 6 for Landsat 5 and 7, and Band 10 for Landsat 8) with the mono-window algorithm. This four-step process is described below.

Step 1: Conversion of Digital Number (DN) to Spectral Radiance

L = ((LMax-LMin)/(QcalMax-QcalMin)) * (DN – Qcalmin) + LMin ……………..…..…….*Equation (1a)*

L = (ML * Qcal) + AL…………….….…………………………………………………………...*Equation (1b)*

Where:

L = spectral radiance,

DN = digital number of each pixel,

LMAX and LMIN = calibration constants,

QCALMAX and QCALMIN = highest and lowest ranges of values for rescaled radiance in DN obtained from the metadata,

ML = band-specific multiplicative scaling factor;

AL = band-specific additive rescaling factor.

Equations (1a) and (1b) apply to Landsat 4/5/7 and Landsat 8, respectively.

Step 2: Conversion of the spectral radiance sensor brightness temperature (TB) using Planck's inverse function.

T = K2 In (K1/(L)+1) -1 …………….….…………………………………………………..….*Equation (2)*

Where:

K1 and K2 = calibration constants for the Landsat image, with K1 values of 607.76, 666.09, and 774.89, and K2 values of 1260.56, 1282.71, and 1321.08 ($W\ m^{-2}\ sr^{-1}\ \mu m^{-1}$) for Landsat TM, ETM+, and OLI/TIRS, respectively.

L = spectral radiance for the thermal band in ($W\ m^{-2}\ sr^{-1}\ \mu m^{-1}$)

Step 3: Calculation of the Land Surface Temperature (LST) in Kelvin

LSTk = T (1 +((L*T)/σ) * In ε)-1…………….…………………………………………..……..*Equation (3)*

where LST = land surface temperature (in Kelvin),

L = wavelength of emitted radiance, which equals 11.5 μm, ρ is h × c/σ (1.438×10^{-2} m K),

h = Planck's constant (6.626×10^{-34} J • s),

c = speed of light (2.998 × 10^8 m/s),

σ = Boltzmann's constant (1.38×10^{-23} J • K^{-1}) — not the Stefan-Boltzmann constant, which is a distinct physical constant used only in the full radiative energy-balance form of the Planck function —

ε = emissivity.

Step 4: Conversion of the Land Surface Temperature (LST) in Kelvin to Celsius

LSTc = LSTk – 273.15…………….……………………………………………………..……..*Equation (4)*

Where:

LSTk = LST in Kelvin calculated in (3)

LSTc = LST in Celsius

2.4 Vegetation Change Detection

To assess changes in the vegetative properties of the study area, the Normalized Difference Vegetation Index (NDVI) will be used. The index uses the Red and Near-Infrared bands of Landsat imagery to assess vegetation health in the area. Therefore, it is calculated as follows:

NDVI= (NIR-R)/(NIR+R) …………….….…………………………………………….….. *Equation (5)*

Where:

NIR = Near Infrared band of the Landsat series (Band 5 for Landsat 8 and Band 4 for Landsat 5 and 7)

R = Red Band (Band 4 for Landsat 8 and Band 3 for Landsat 5 and 7)

3. RESULTS AND DISCUSSION

3.1 Land use and land cover change for the past 30 years

Land use and land cover changes in the area have been observed over the past 30 years. Due to the continuous increase in urban settlements, several changes have been observed in other land-use and land-cover types within the study area (Figures 2 & 3). In 1991, Light Vegetation was the predominant land use and land cover type, covering over 40% of the study area, while settlements were the least, covering just about 7%, as shown in Table 1.

Table 1. Area (Km^2 and %) covered by each land use/land cover change within the study area for the past 30 years.

	1991		**2001**		**2011**		**2021**	
	Area (km^2)	**Area (%)**	**Area (km^2)**	**Area (%)**	**Area (km^2)**	**Area (%)**	**Area (km^2)**	**Area (%)**
Settlements	4.25	7.69	7.22	13.05	11.59	20.94	17.95	32.42
Thick Vegetation	16.90	30.53	17.68	31.95	21.29	38.46	22.08	39.90
Light Vegetation	22.57	40.77	23.66	42.75	19.35	34.97	13.65	24.65
Rivers	11.63	21.02	6.78	12.25	3.12	5.64	1.68	3.03

Thirty years later, in 2021, Light Vegetation had decreased to 24% of the study area, while settlements that had initially occupied a small share of the area had expanded to over 32%. This represents more than a fourfold increase in settlement area over the study period, reflecting rapid urban expansion within Osogbo Local Government Area.

It is also observed in Table 1 that Thick Vegetation cover increased from 30.53% in 1991 to 39.90% in 2021, even as Light Vegetation cover and River/surface-water area both declined substantially over the same period. This apparent increase in Thick Vegetation area, considered alongside the overall decline in NDVI values discussed in Section 3.3, indicates that gains in vegetated area were not accompanied by corresponding gains in vegetation vigour, and that the classification scheme used here captures canopy density/cover rather than vegetation health directly. Similarly, the notable reduction of river/surface-water area, from 21.02% in 1991 to 3.03% in 2021, is attributed principally to encroachment of settlement and vegetation onto the floodplain and river banks, compounded by the seasonally low water levels associated with the dry-season (December-January) image-acquisition window used for all four epochs, rather than to a permanent physical loss of the water body.

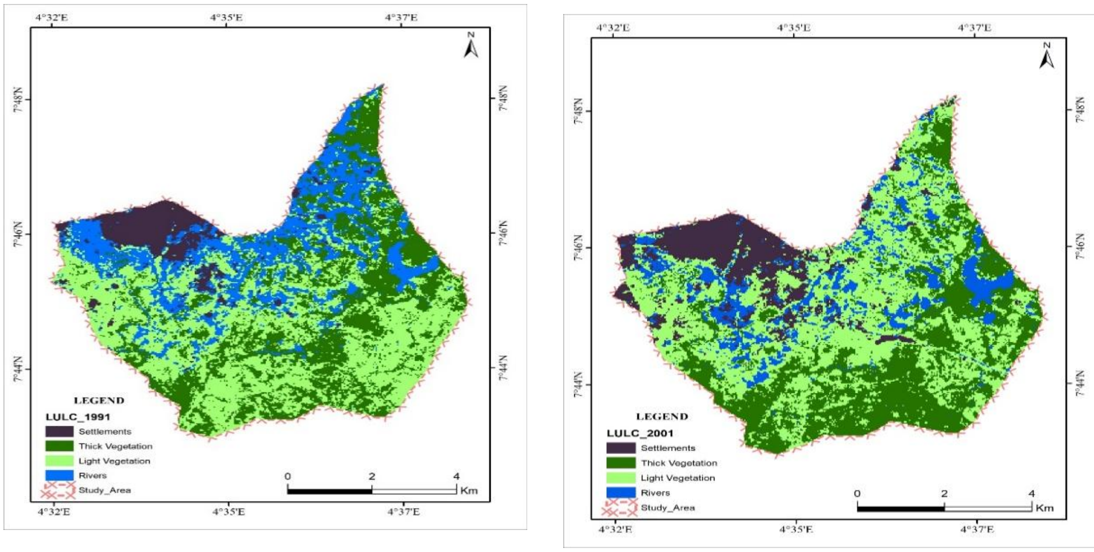

Figure 2. Land use and land cover change for the years 1991 and 2001

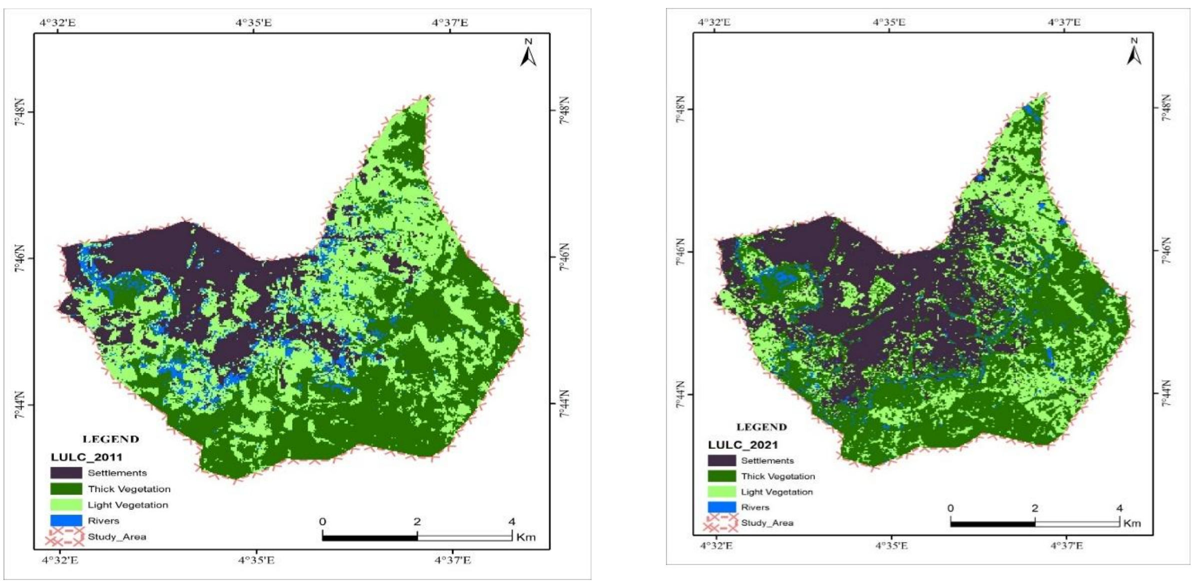

Figure 3. Land use and land cover change for the years 2011 and 2021

3.2 Land Surface Temperature (LST) Change

The LST change in the study area over the last 30 years, as shown in Figures 4 and 5, indicates significant variations in temperature levels within the region. A detailed look at the temperature distribution reveals a consistent increase in temperatures in the areas occupied by settlements compared to other features. For example, in 1991, the average temperature in settlement areas ranged from 19.1°C to 20.8°C, whereas by 2021 it had risen to 27.7°C to 30.1°C. The trend of LST and its relationship with NDVI and other LULC features is discussed in another section of this article. Overall, it can be concluded that LST continues to rise with increasing settlement numbers in the study area.

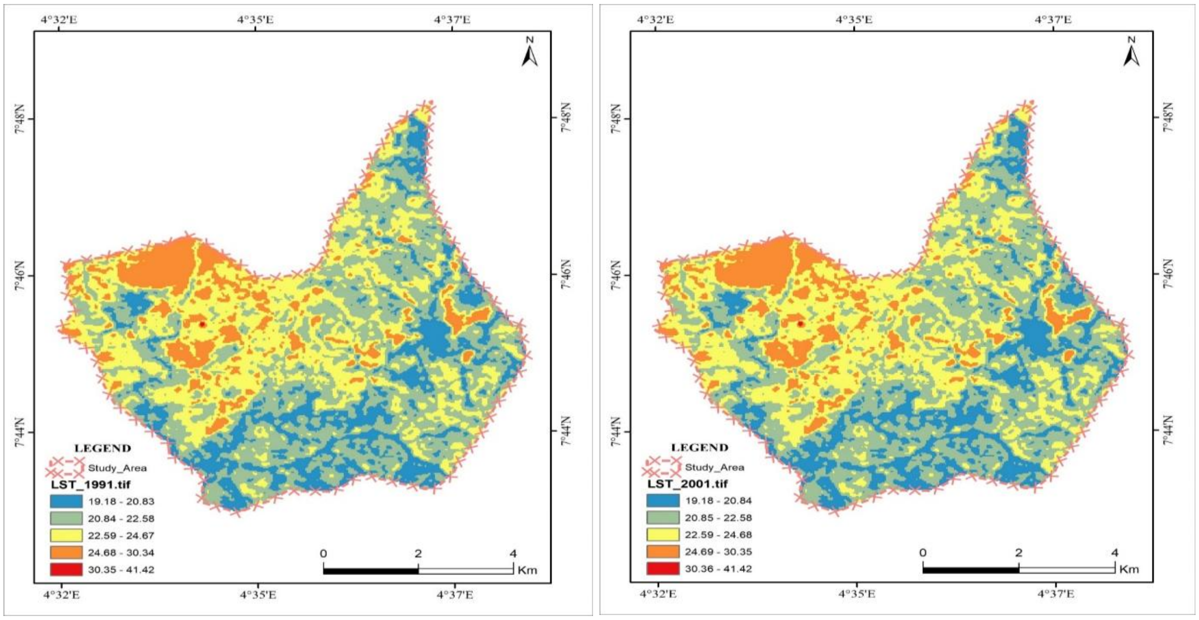

Figure 4. Land Surface Temperature Change for the years 1991 and 2001

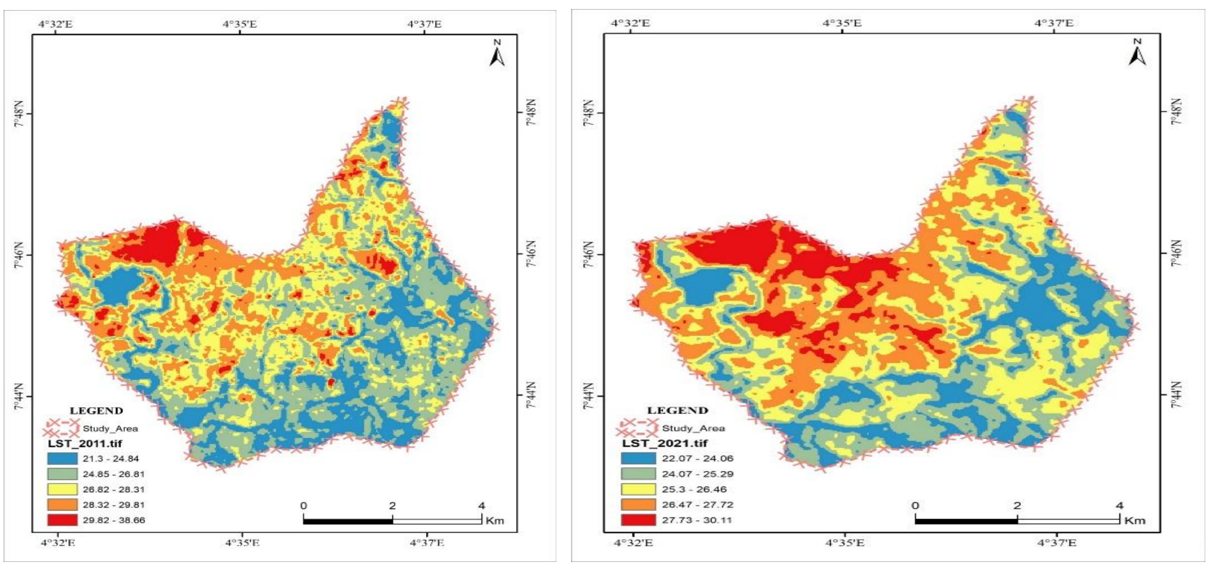

Figure 5. Land Surface Temperature Change for the years 2011 and 2021.

3.3 Normalized Difference Vegetative Index (NDVI) Change

Figures 6 and 7 show changes in NDVI values in the study area over the past 30 years. It was observed that NDVI, which had its highest value of 0.429 at the beginning of the study in 1991, decreased to 0.355 by 2021, at the end of the study period. Because this decline occurred even as total vegetated area (Thick Vegetation plus Light Vegetation) remained broadly stable, it indicates a decline in vegetation health and vigour, rather than in the extent of vegetation cover, within the study area.

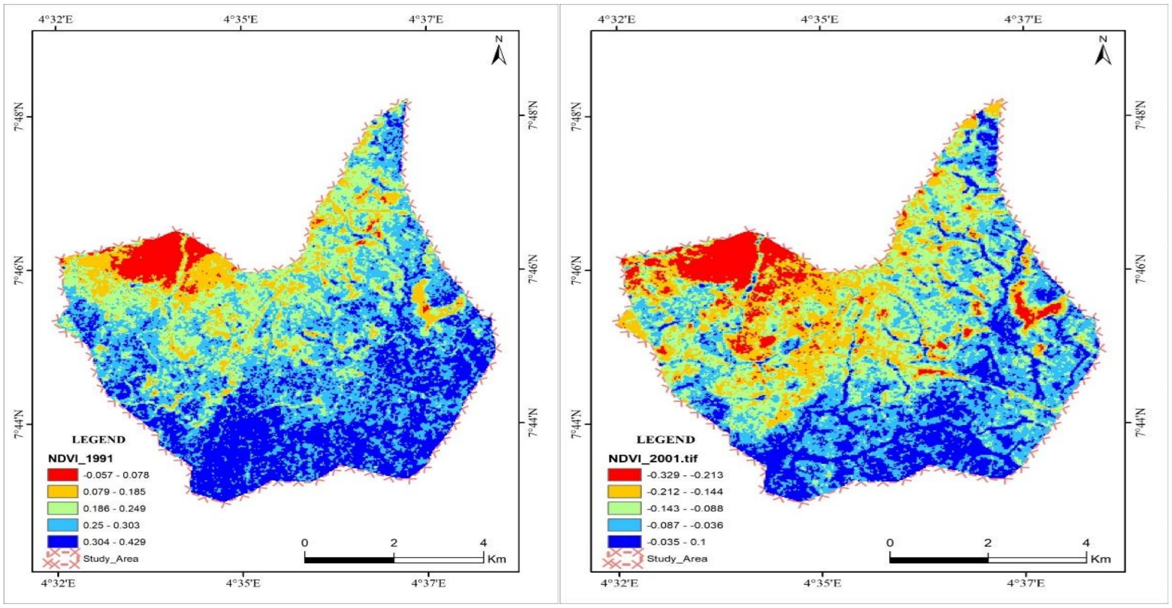

Figure 1. NDVI change of the study area for the years 1991 and 2001

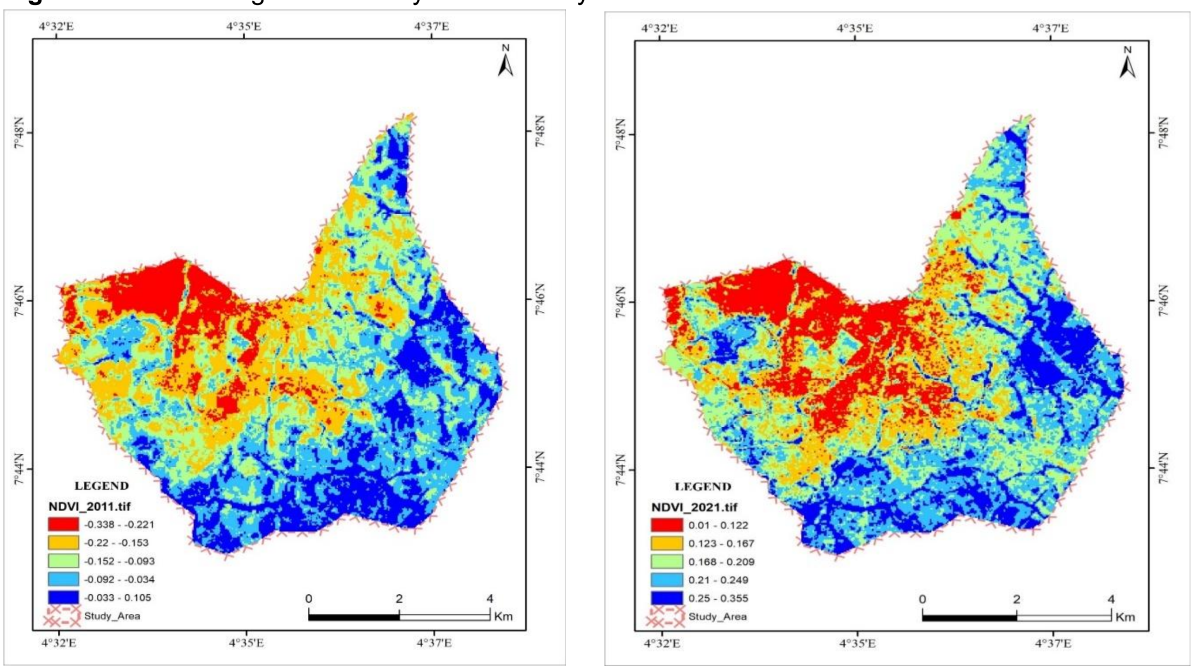

Figure 2. NDVI change of the study area for the year 2011 and 2021.

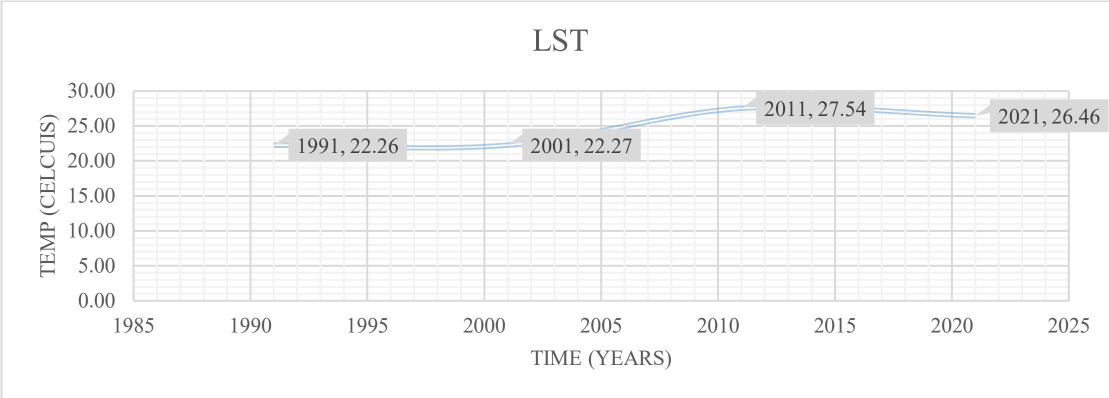

Figure 8. Trend of the average value of the LST within the study area for the past 30 years

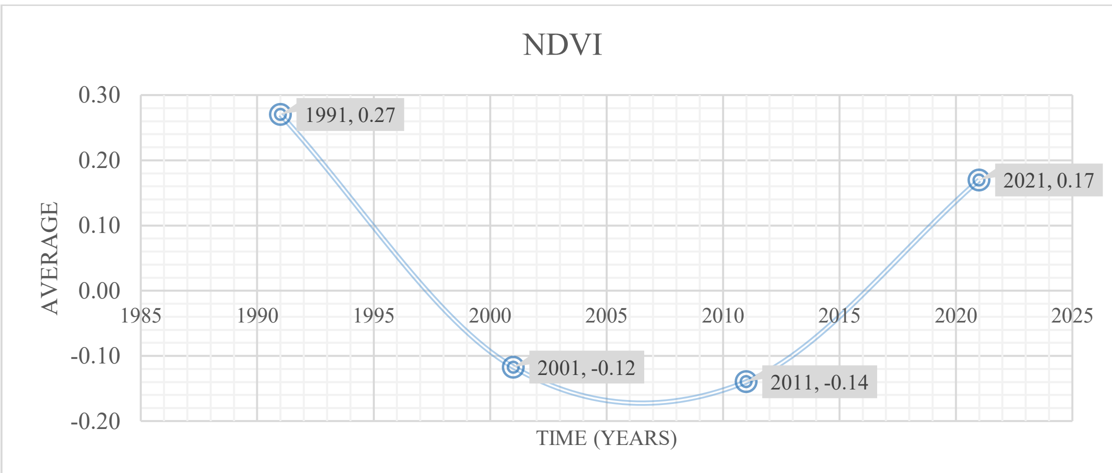

Figure 9. Trend of the average value of the NDVI within the study area for the past 30 years

The average NDVI and LST show a very weak negative correlation, with a correlation coefficient of -0.27.

3.4 Relationship Between LST, NDVI, And LULC

The relationships among the LST, NDVI, and LULC within the study area, as shown in Tables 2-5, indicate that the LST has a very strong positive correlation with Settlements, with a value of 0.80, while the NDVI has a very weak negative correlation with Settlements, with a value of -0.04. This implies that although the LST of Osogbo increases due to an increase in Settlements, this change will have little or no effect on the vegetation health within the study area. Although there is an increase in Thick Vegetation in this area, the NDVI-Thick Vegetation correlation is very weak, implying that although there is growth in the Vegetation, it is not as healthy as it should be.

The direction of the Settlement-LST relationship observed in Osogbo (a strong positive association) is consistent with the pattern reported for other rapidly urbanising Nigerian cities, including Lagos Metropolis (Babalola & Akinsanola, 2016), Ibadan (Fashae et al., 2020), and Benin City (Fabolude & Aighewi, 2022), reinforcing the broader conclusion that unmanaged settlement expansion is a consistent driver of surface warming across similarly sized Nigerian urban centres, even though the exact magnitude of the effect varies with local urban structure and climate.

Table 2. Relationship between the settlements, LST, and NDVI within the study area

R	Settlements	LST	NDVI
Settlements	1.00	0.80	-0.04
LST	0.80	1.00	-0.27
NDVI	-0.04	-0.27	1.00

Table 3. Relationship between the Thick Vegetation, LST, and NDVI within the study area

R	Thick Vegetation	LST	NDVI
Thick Vegetation	1.00	0.95	-0.19
LST	0.95	1.00	-0.27
NDVI	-0.19	-0.27	1.00

Table 4. Relationship between the Light Vegetation, LST, and NDVI within the study area

R	Light Vegetation	LST	NDVI
Light Vegetation	1.00	-0.05	-0.93
LST	-0.05	1.00	-0.27
NDVI	-0.93	-0.27	1.00

Table 5. Relationship between the River, LST, and NDVI within the study area

R	River	LST	NDVI
River	1.00	-0.85	0.41
LST	-0.85	1.00	-0.27
NDVI	0.41	-0.27	1.00

Source: Author's work (2026)

4. CONCLUSION

This study examined the effects of changes in land use and land cover within Osogbo Local Government on both temperature and vegetation. Landsat imagery was used to conduct the analysis, with Land Surface Temperature (LST) as the measure of temperature change and the Normalized Difference Vegetation Index (NDVI) as the measure of vegetation change and health status within the study area. It was observed that there was a continuous increase in settlement area within the study area, with the effect most evident along the river corridor. The LST showed a continuous increase, especially in areas with increasing settlement, while the average NDVI showed a continuous decline. The correlation between LST, settlements, and NDVI shows a very strong positive correlation between LST and settlements (r = 0.80), while a very weak negative correlation exists between NDVI and settlements (r = -0.04) within the study area. Correlation analysis of the individual vegetation classes further shows that although Thick Vegetation cover increased over the study period, its relationship with NDVI remained weak (r = -0.19), whereas the declining Light Vegetation cover showed a strong negative correlation with NDVI (r = -0.93), suggesting that the observed gains in vegetated area were not matched by corresponding gains in vegetation health. This decline in vegetation health may be partly attributable to the dry-season (January) timing of the image acquisitions used in this study, and future work using wet-season imagery is recommended to confirm the extent of the observed decline.

While declining vegetation health in rapidly urbanising areas can arise from multiple pressures, including soil sealing, reduced infiltration, and localised air-quality changes associated with traffic and small-scale industrial activity, this study did not directly measure air-quality or industrial-emission parameters; any attribution of the observed decline to industrial gas emissions should therefore be treated as a hypothesis for future investigation rather than as a confirmed finding of this study. Hence, further action should be taken to ensure the preservation of both vegetation and water resources within the study area to sustain future generations.

Specifically, it is recommended that: (i) an environmental impact assessment be conducted before further construction within the study area; (ii) the development of buildings on river banks and floodplains be discouraged, and existing riparian vegetation buffers be protected and, where degraded, restored; (iii) urban greening programmes, including street-tree planting and the deliberate protection of remaining Thick Vegetation patches, be incorporated into Osogbo's land-use planning framework; and (iv) periodic air-quality monitoring be instituted in areas of concentrated industrial and vehicular activity to establish empirically whether a measurable link exists between local emissions and the observed vegetation decline.

REFERENCE

Arnfield, A. J. (2003). Two decades of urban climate research: A review of turbulence, exchanges of energy and water, and the urban heat island. International Journal of Climatology, 23(1), 1–26. https://doi.org/10.1002/joc.859

Babalola, O. S., & Akinsanola, A. A. (2016). Change detection in land surface temperature and land use land cover over Lagos Metropolis, Nigeria. Journal of Remote Sensing & GIS, 5(2), 171. https://doi.org/10.4172/2469-4134.1000171

Becker, F., & Li, Z.-L. (1990). Temperature-independent spectral indices in thermal infrared bands. Remote Sensing of Environment, 32(1), 17–33. https://doi.org/10.1016/0034-4257(90)90095-4

Cai, Y., Zhang, H., Zheng, P., & Pan, W. (2016). Quantifying the impact of land use/land cover changes on the urban heat island: A case study of the natural wetlands distribution area of Fuzhou City, China. Wetlands, 36, 285–298. https://doi.org/10.1007/s13157-016-0738-7

Chander, G., Markham, B. L., & Helder, D. L. (2009). Summary of current radiometric calibration coefficients for Landsat MSS, TM, ETM+, and EO-1 ALI sensors. Remote Sensing of Environment, 113(5), 893–903. https://doi.org/10.1016/j.rse.2009.01.007

Du, C., Ren, H., Qin, Q., Meng, J., & Zhao, S. (2015). A practical split-window algorithm for estimating land surface temperature from Landsat 8 data. Remote Sensing, 7(1), 647–665. https://doi.org/10.3390/rs70100647

Fabolude, G., & Aighewi, I. T. (2022). Evaluation of the extent of land use-land cover changes of Benin City, Edo State, Nigeria from 1987–2019. Journal of Applied Sciences and Environmental Management, 26(8), 1443–1450. https://doi.org/10.4314/jasem.v26i8.18

Fashae, O. A., Olusola, A. O., & Ayanshola, A. M. (2020). Urban heat island and land use/land cover change detection using NDVI and LST in Ibadan, Nigeria. Environmental Monitoring and Assessment, 192(11), 703. https://doi.org/10.1007/s10661-020-08630-0

Guha, S., Govil, H., Dey, A., & Gill, N. (2018). Analytical study of land surface temperature with NDVI and NDBI using Landsat 8 OLI and TIRS data in Florence and Naples city, Italy. European Journal of Remote Sensing, 51(1), 667–678. https://doi.org/10.1080/22797254.2018.1474494

Karnieli, A., Agam, N., Pinker, R. T., Anderson, M., Imhoff, M. L., Gutman, G. G., Panov, N., & Goldberg, A. (2010). Use of NDVI and land surface temperature for drought assessment: Merits and limitations. Journal of Climate, 23(3), 618–633. https://doi.org/10.1175/2009JCLI2900.1

Nega, W., & Balew, A. (2022). The relationship between land use, land cover and land surface temperature using remote sensing: Systematic reviews of studies globally over the past 5 years. Environmental Science and Pollution Research, 29, 42493–42508. https://doi.org/10.1007/s11356-022-19997-z

Olorunfemi, I. E., Fasinmirin, J. T., Olufayo, A. A., & Komolafe, A. A. (2018). GIS and remote sensing-based analysis of the impacts of land use/land cover change (LULCC) on the environmental sustainability of Ekiti State, southwestern Nigeria. Environment, Development and Sustainability. https://doi.org/10.1007/s10668-018-0214-z

Parlow, E. (2021). Regarding some pitfalls in urban heat island studies using remote sensing technology. Remote Sensing, 13(18), 3598. https://doi.org/10.3390/rs13183598

Shi, H., Xian, G., Auch, R., Gallo, K., & Zhou, Q. (2021). Urban heat island and its regional impacts using remotely sensed thermal data—A review of recent developments and methodology. Land, 10(8), 867. https://doi.org/10.3390/land10080867

Stewart, I. D., Krayenhoff, E. S., Voogt, J. A., Lachapelle, J. A., Allen, M. A., & Broadbent, A. M. (2021). Time evolution of the surface urban heat island. Earth's Future, 9(10), e2021EF002178. https://doi.org/10.1029/2021EF002178

Voogt, J. A., & Oke, T. R. (2003). Thermal remote sensing of urban climates. Remote Sensing of Environment, 86(3), 370–384. https://doi.org/10.1016/S0034-4257(03)00079-8

Weng, Q. (2001). A remote sensing-GIS evaluation of urban expansion and its impact on surface temperature in the Zhujiang Delta, China. International Journal of Remote Sensing, 22(10), 1999–2014. https://doi.org/10.1080/713860788

Weng, Q. (2003). Fractal analysis of satellite-detected urban heat island effect. Photogrammetric Engineering and Remote Sensing, 69(5), 555–566. https://doi.org/10.14358/PERS.69.5.555

Weng, Q., Lu, D., & Schubring, J. (2004). Estimation of land surface temperature–vegetation abundance relationship for urban heat island studies. Remote Sensing of Environment, 89(4), 467–483. https://doi.org/10.1016/j.rse.2003.11.005

Weng, Q., Liu, H., & Lu, D. (2007). Assessing the effects of land use and land cover patterns on thermal conditions using landscape metrics in city of Indianapolis, United States. Urban Ecosystems, 10(2), 203–219. https://doi.org/10.1007/s11252-007-0020-0

Yu, X., Guo, X., & Wu, Z. (2014). Land surface temperature retrieval from Landsat 8 TIRS—Comparison between radiative transfer equation-based method, split window algorithm and single channel method. Remote Sensing, 6(10), 9829–9852. https://doi.org/10.3390/rs6109829

Zha, Y., Gao, J., & Ni, S. (2003). Use of normalized difference built-up index in automatically mapping urban areas from TM imagery. International Journal of Remote Sensing, 24(3), 583–594. https://doi.org/10.1080/01431160304987